

Ising model on the aperiodic Smith hat

Yutaka Okabe¹, Komajiro Niizeki^{2†} and Yoshiaki Araki³

¹Department of Physics, Tokyo Metropolitan University, Hachioji, Tokyo 192-0397, Japan

²Graduate School of Science, Tohoku University, Aoba-ku, Sendai 980-8578, Japan

³Japan Tessellation Design Association, Musashino-shi, Tokyo 180-0003, Japan

E-mail: okabe@phys.se.tmu.ac.jp

5 March 2024

Abstract. Smith *et al* discovered an aperiodic monotile of 13-sided shape in 2023. It is called the ‘Smith hat’ and consists of 8 kites. We deal with the statistical physics of the lattice of the kites, which we call the ‘Smith-kite lattice’. We studied the Ising model on the aperiodic Smith-kite lattice and the dual Smith-kite lattice using Monte Carlo simulations. We combined the Swendsen-Wang multi-cluster algorithm and the replica exchange method. We simulated systems up to the total spin number 939201. Using the finite-size scaling analysis, we estimated the critical temperature on the Smith-kite lattice as $T_c/J = 2.405 \pm 0.0005$ and that of the dual Smith-kite lattice as $T_c^*/J = 2.143 \pm 0.0005$. Moreover, we confirmed the duality relation between the critical temperatures on the dual pair of aperiodic lattices, $\sinh(2J/T_c) \sinh(2J/T_c^*) = 1.000 \pm 0.001$. We also checked the duality relation for the nearest-neighbor correlation at the critical temperature, essentially the energy, $\epsilon(T_c)/\coth(2J/T_c) + \epsilon(T_c^*)/\coth(2J/T_c^*) = 1.000 \pm 0.001$.

Keywords: Smith hat, aperiodic lattice, Ising model, Monte Carlo simulation, duality relation

† Professor emeritus

1. Introduction

It is possible to fill a two-dimensional plane with a single shape using regular polygons: equilateral triangles, squares, and regular hexagons. It has long been a matter of interest to determine whether there are other shapes. Penrose [1] showed that a plane can be filled with two shapes, a fat rhombus and a thin rhombus, where the golden ratio, an irrational number, is involved. The tilings obtained from these shapes do not have the usual periodic structure but creates a quasiperiodic structure. It exhibits the 5-fold (10-fold) symmetry. The quasicrystal [2] was studied by experimental studies, and Shechtman *et al* discovered the 5-fold (10-fold) symmetry [3]. The Nobel Prize in Chemistry 2011 was awarded to Shechtman “for the discovery of quasicrystals”.

Smith, Myers, Kaplan and Goodman-Strauss discovered an aperiodic monotile in 2023 [4]. The shape is 13-sided and called the ‘hat’. It is able to fill an infinite plane without overlaps or gaps in a pattern that not only never repeats but also never can be repeated. Various studies have been conducted following this discovery [5, 6, 7, 8]. In [6] and [7], the vertex set of the monotile is shown to be a two-dimensional quasiperiodic lattice (2DQL) which is obtained from a six-dimensional or a four-dimensional periodic lattice by the cut-and-projection method. 2DQLs are divided into two groups according to the nature of the projection window used in the cut-and-projection method. The window of a 2DQL belonging to one of the two groups is a polygon but the one belonging to the other group is a domain with a fractal boundary. A representative 2DQL of the first group is Penrose tiling P1, whose major tile is a regular pentagon. The monotile is shown, however, to belong to the second group [6, 7].

The material science of quasilattices has been studied experimentally and theoretically in various ways. Recent studies have focused on superconductivity [9, 10], electric structure [11] and magnetic properties [12]. There has been much interest in the phase transitions of spin systems on quasicrystals compared to those of ordered and random systems. Okabe and Niizeki [13] studied spin systems on a Penrose lattice mainly by means of Monte Carlo simulation. They showed that the Ising model on the Penrose lattice belongs to the same universality class as that on the two-dimensional (2D) regular lattice. In addition, they studied the dual lattice [14] and discussed the duality relation. A high-precision study was performed recently up to $N = 20,633,239$ using a GPU-based calculation [15]; A significant improvement in accuracy was obtained.

In contrast, no one has investigated up to present spin systems on a 2DQL belonging to one of the second group in the classification above. In this paper, we study the Ising models on the Smith-kite lattice and its dual lattice by means of the Monte Carlo simulation. We use the Swendsen-Wang (SW) multi-cluster spin-flip algorithm [16] combined with the replica exchange method of parallel tempering [17]. We organize the rest of the paper as follows. In Sec. 2, we explain the model and numerical method. We give the results in Sec. 3. We report the estimate of the critical temperature, and discuss the duality relation. The final section is devoted to the summary and discussions.

2. Model and Numerical Method

2.1. Lattice

Smith, Myers, Kaplan and Goodman-Strauss announced the discovery of an aperiodic monotile in March 2023 [4]. This brand new 13-sided shape is called ‘the Smith hat’. We here study statistical physics of spin systems on the Smith-hat tiling. As for the coordinate data, we use the code released by Cheritat [18], which is a web application written in JavaScript. The 4-dimensional coordinate data of the hat vertices are given there, and by projecting them into two dimensions, 2-dimensional coordinate data can be obtained. Cheritat provides four sizes of Smith-hat tiling data. The number of hats is 357, 2490, 17077 and 117051 for “small”, “medium”, “big” and “bigger” hat tiling, respectively. The Smith-hat tiling of the “small” size is illustrated in figure 1. It is noteworthy to mention a family of aperiodic monotiles [4]. The notation $\text{Tile}(a, b)$, where a and b are real numbers, is used to specify a shape of hat tile. $\text{Tile}(1, \sqrt{3})$, which is the most popular, has 8 kites in the hat, whereas $\text{Tile}(\sqrt{3}, 1)$ has 10 kites in the hat. Although we mainly treat $\text{Tile}(1, \sqrt{3})$ of a 13-sided monotile with 8 kites in this paper, we show both $\text{Tile}(1, \sqrt{3})$ and $\text{Tile}(\sqrt{3}, 1)$ in figure 1. In the site of Cheritat [18], the default value of α_1 is provided as 60 for $\text{Tile}(1, \sqrt{3})$. When we treat $\text{Tile}(\sqrt{3}, 1)$, we set α_1 as 30.

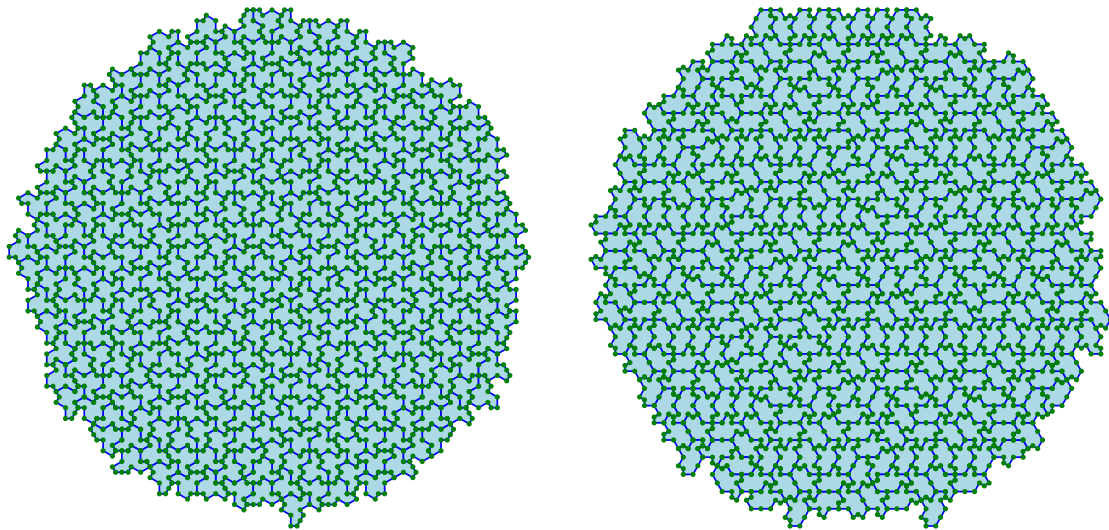


Figure 1. Smith-hat tiling of the “small” size ($N_{\text{hat}} = 357$). We use the code released by Cheritat [18]. The left illustration is $\text{Tile}(1, \sqrt{3})$ of 8 kites, whereas the right illustration is $\text{Tile}(\sqrt{3}, 1)$ of 10 kites.

We consider the lattice based on the kites. A hat consists of 8 or 10 kites. The vertices of the kites become the lattice points. There are extra 2 (4) lattice points in an 8-kite (10-kite) hat. We need the information on the connection of kite vertices; we make a table of connecting sites by checking the vertices shared by neighboring hats. One vertex is shared by two, three or four hats. In this way, we form a lattice made by

the vertices of the kites, and we call it the original Smith-kite lattice. We also consider the dual lattice, which we call the dual Smith-kite lattice. The lattice points of the dual lattice are set in a kite. We make the connection between the dual lattice points by the two adjacent kites. These two lattices are dual, and we will examine the duality relations for dual lattices discussed by Kramers and Wannier [19]. The original and dual Smith-kite lattices are illustrated in figure 2. The lattice points of the original lattice are denoted by green circles, whereas those of the dual lattice are denoted by empty red circles. The edges of the dual lattice are denoted by red dotted lines. We put spins on the lattice points when we study the Ising model.

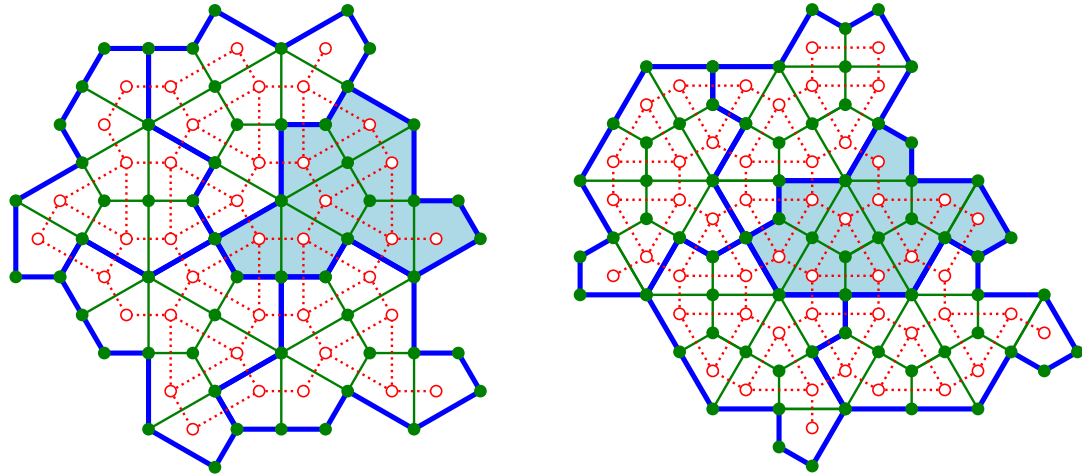


Figure 2. Smith-kite lattices. The left panel is $\text{Tile}(1, \sqrt{3})$ of 8 kites, whereas the right panel is $\text{Tile}(\sqrt{3}, 1)$ of 10 kites. The edges of the Smith hat are denoted by blue lines. One hat is denoted by a shaded area. A hat consists of 8 or 10 kites, and the edges of the kites are denoted by thin green lines, which form the original Smith-kite lattice. The lattice points of the original Smith-kite lattice are denoted by green circles, whereas those of the dual Smith-kite lattice are denoted by empty red circles. We can see that there are extra 2 (4) lattice points in one 8-kite (10-kite) hat. The edges of the dual lattice are denoted by red dotted lines. In the Ising model, spins are put on the lattice points.

The sizes of the lattices are tabulated in table 1. This is the data for $\text{Tile}(1, \sqrt{3})$ of 8 kites. The second column gives the number of hats for four sizes. The number of center of kites is 8 times the number of hats, whereas the number of vertex of kites is slightly larger because of the boundary. When we discuss the averaged values for the spins in the simulation, it is better to take an average over only inner sites, in order to reduce surface effects. Thus, we also list the number of inner spins.

2.2. Model and simulation

We deal with the Hamiltonian of the Ising model given by

$$\mathcal{H} = -J \sum_{\langle i,j \rangle} s_i s_j, \quad s_i = \pm 1, \quad (1)$$

Table 1. Size of Smith-hat tiling provided by Cheritat [18]. This is the data for $\text{Tile}(1, \sqrt{3})$ of 8 kites. The original Smith-kite lattice is formed by the vertex of kites, whereas the dual Smith-kite lattice is formed by the center of kites. The number of the inner sites will be used when taking an average in the simulation, and it will be denoted by N .

	hats	vertex of kites		center of kites	
		total	inner	total	inner
“small”	357	3011	2807	2856	2655
“medium”	2490	20388	19794	19920	19372
“big”	17077	137686	136266	136616	135216
“bigger”	117051	939201	935529	936048	932721

where J is the coupling and s_i is the spin at lattice site i . The lengths of the bonds in the kite are not all equal; since we are discussing the network structure of the lattice, we assume that the interaction constants all take constant J . The summation is taken over nearest-neighbor pairs $\langle i, j \rangle$. Here, we consider the case of the ferromagnetic coupling ($J > 0$).

In performing the Monte Carlo simulation, we employ the multi-cluster spin-flip SW algorithm [16] to escape from the problem of the long autocorrelation time near the critical temperature. We also combine the replica exchange method of parallel tempering [17]. We used the 20,000 Monte Carlo steps (MCS) after discarding the first 2,000 MCS for the “small” and “medium” sizes. We used the 10,000 MCS after the first 1,000 MCS for the “big” size, and the 5,000 MCS after the 500 MCS for the “bigger” size. Since the cluster flip algorithm [16] is used, the time required for equilibration is very short. Even for a largest system size, 100 steps are sufficient for equilibration. We discarded 1/10th of the measurement time steps. For temperature dependence, precise measurement is possible by applying the replica exchange method [17]. As the system size increases, it becomes necessary to take a narrower temperature difference to exchange temperatures. The detailed balance conditions are fulfilled for both algorithms. We made five independent runs with different random number sequences for each size to estimate numerical errors. In most plots the error bars are within the size of the marks. This study dealt with a sample of one configuration for each size. Because we are cutting finite sizes from an infinite system, we can take some other configurations. However, since we are dealing with sufficiently large sizes, we expect the dependence on configuration to be very small.

We make the Monte Carlo updates for the spins on all the sites. However, we take the average of physical quantities over only the spins on inner sites to reduce surface effects. Surface effects are one of the important topics in the study of critical phenomena, and numerical investigation of surface effects is often performed based on the difference between periodic and free boundary conditions [20]. In this study, the bulk properties

are the main subject, and we will consider the quantity excluding the surface layer. The number of the inner sites for both original and dual lattices are tabulated in table 1, and in the following, we denote N for the number of inner sites.

3. Results

3.1. Results of magnetization

We present the simulation results of $\text{Tile}(1, \sqrt{3})$ of 8 kites. We first show the results of the magnetization per spin, $m = (1/N) \sum_i M_i$. We plot the temperature dependence of the squared magnetization, $\langle m^2 \rangle$, in figure 3. We show the data of the four sizes, “small”, “medium”, “big”, and “bigger”, for both original and dual lattices. The temperature is measured in units of J , that is, $J = 1$. In figure 3, we observe the spontaneous magnetization for lower temperature.

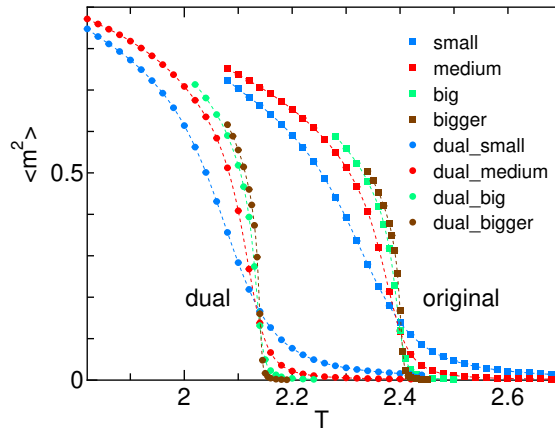


Figure 3. Squared magnetization of the Ising model on the Smith-kite lattices for both original and dual lattices.

Binder [21] pointed out that the moment ratio is effective for locating the critical temperature based on the finite-size scaling (FSS) analysis. We plot the temperature dependence of the moment ratio $\langle m^4 \rangle / \langle m^2 \rangle^2$ in figure 4. We give the data of four sizes for both original and dual lattices. This value approaches 1 for the ordered state ($T \rightarrow 0$), and approaches 3 for the disordered state ($T \rightarrow \infty$) because of Gaussian fluctuations.

The correlation length ξ diverges as the temperature approaches the critical temperature as

$$\xi(T) \propto |T - T_c|^{-\nu} \quad (2)$$

with the correlation-length exponent ν . The FSS [22, 23] postulates that near the critical temperature the physical quantities of finite systems with the linear size L are scaled by ξ/L . The magnetization scales as

$$\langle m^2 \rangle = L^{-2\beta/\nu} f(tL^{1/\nu}), \quad (3)$$

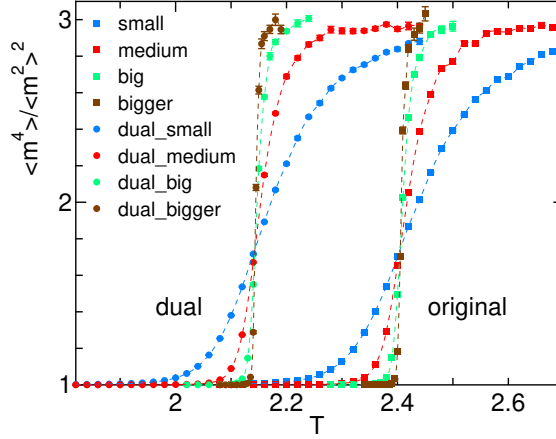


Figure 4. Moment ratio of the Ising model on the Smith-kite lattices for both original and dual lattices.

where β is the spontaneous-magnetization exponent and $t = T - T_c$. Then, the moment ratio becomes a single scaling variable such that

$$\langle m^4 \rangle / \langle m^2 \rangle^2 = \tilde{f}(tL^{1/\nu}). \quad (4)$$

It means that the plots $\langle m^4 \rangle / \langle m^2 \rangle^2$ of various sizes intersect at a single point, which leads to the estimate of the critical temperature. It is to be noted that there are corrections to FSS for small sizes. We see the crossing of data of different sizes in figure 4. We here make a comment on the error bars. At very high temperatures, this ratio becomes a 0/0 quantity, so the error bars may become large. However, just above the critical point, the error is still small even for the largest system size.

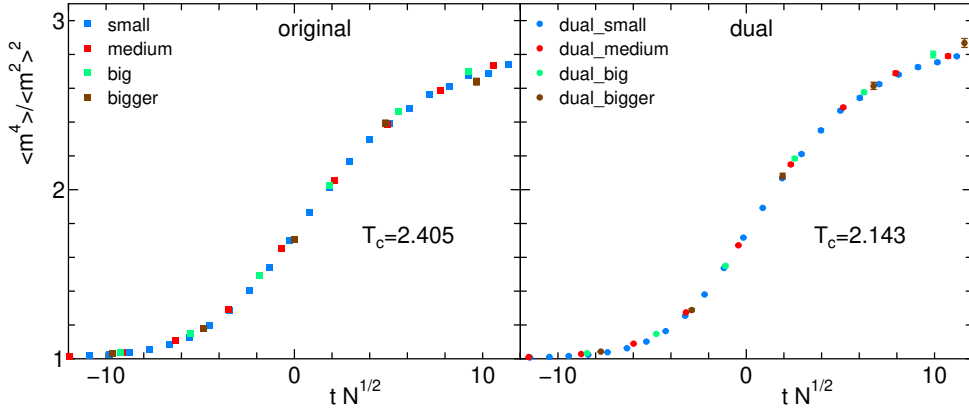


Figure 5. FSS of moment ratio for the Ising model on the Smith-kite lattices; $t = T - T_c$ and $\nu = 1$. The left panel is the FSS plot for the original lattice, where we assume $T_c = 2.405$, whereas the right panel is that for the dual lattice, where we assume $T_c^* = 2.143$.

Assuming the critical temperature T_c , we try the FSS plots for both original and dual lattices in figure 5. The linear size L is $N^{1/2}$, and we use $\nu = 1$ of the 2D Ising

value of the regular lattice. The universality of the critical exponents for quasiperiodic spin systems has been confirmed, and even if we analyze the critical exponent as a fitting parameter, we will obtain almost the same value as the exact solution using the FSS analysis. The left panel is the FSS plot for the original lattice, where we assume $T_c = 2.405$, whereas the right panel is that for the dual lattice, where we assume $T_c^* = 2.143$.

For comparison, in figure 6 we show the FSS trial when T_c is assumed to be 2.404 and 2.406 in the case of the original lattice. For clarity, we use larger marks for the “bigger” lattice. If you compare figure 6 with the left panel of figure 5, we can see that $T_c = 2.405$ is a good choice. The trial plots of $T_c = 2.404$ and $T_c = 2.406$ in figure 6 are choices of data to highlight the differences. We can obtain an estimate of the error in the narrow interval. Thus, our estimates of the critical temperatures are

$$\text{original lattice } T_c = 2.405 \pm 0.0005 \quad (5)$$

and

$$\text{dual lattice } T_c^* = 2.143 \pm 0.0005. \quad (6)$$

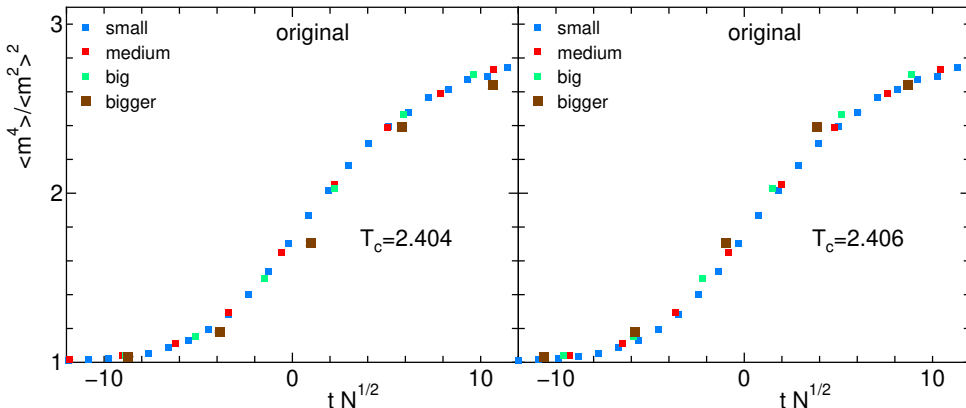


Figure 6. FSS trial of moment ratio for the Ising model on the original Smith-kite lattices. Choose $T_c = 2.404$ (left panel) and $T_c = 2.406$ (right panel). For clarity, larger marks are used for the “bigger” lattice.

Next, we show the FSS of magnetization, (3), in figure 7. Here, the critical exponents are those of the regular lattice, $\nu = 1$ and $\beta = 1/8$, and T_c are chosen as the values of (5) and (6). From figure 7, we can see that the FSS works quite well.

We now consider the duality relation. A simple relation is known between the partition functions of the Ising models on a regular lattice and its dual lattice [19, 24]. The duality relation between the critical temperatures, T_c and T_c^* , is given by

$$\sinh(2J/T_c) \sinh(2J/T_c^*) = 1. \quad (7)$$

Substituting the estimates of the critical temperatures on the Smith-kite lattice (5), and its dual lattice, (6), we obtain $\sinh(2/T_c) \sinh(2/T_c^*) = 1.000 \pm 0.001$. The duality relation is well satisfied for the aperiodic monotile lattice.

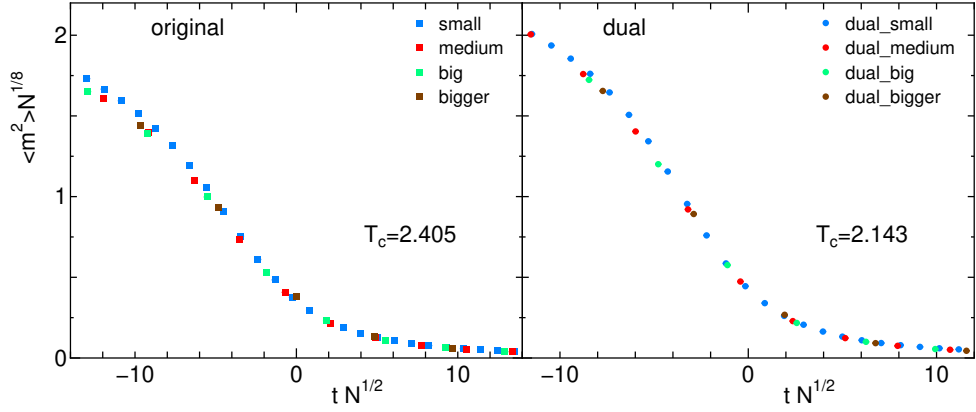


Figure 7. FSS of magnetization for the Ising model on the Smith-kite lattice; $t = T - T_c$, $\nu = 1$ and $\beta = 1/8$. The left panel is the FSS plot for the original lattice, where we assume $T_c = 2.405$, whereas the right panel is that for the dual lattice, where we assume $T_c^* = 2.143$.

3.2. Results of Energy

Another check of the duality is the duality relation for the critical energy,

$$\frac{\epsilon(T_c)}{\coth(2J/T_c)} + \frac{\epsilon(T_c^*)}{\coth(2J/T_c^*)} = 1, \quad (8)$$

where $\epsilon(T_c)$ is the nearest neighbor spin correlation at the critical temperature. This quantity is related to the energy per spin at the critical temperature by $\epsilon(T_c) = -E(T_c)/2N$.

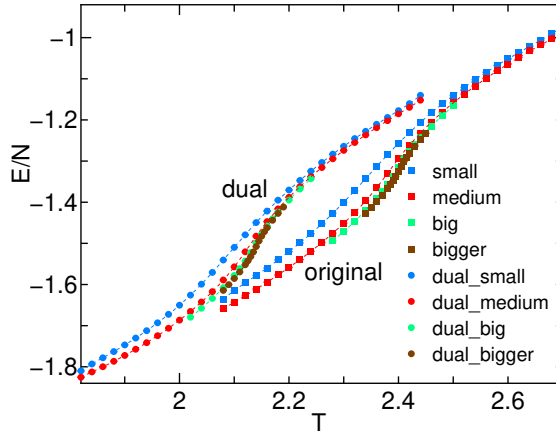


Figure 8. Energy of the Ising model on the Smith-kite lattices for both original and dual lattices.

The temperature dependence of the energy of the Ising model on the Smith-kite lattice and its dual lattice is shown in figure 8. In order to estimate the energy at the critical temperature, we use the FSS for the critical energy, $(E(T_c, L) - E(T_c))/N \propto$

$tL^{-(1-\alpha)/\nu}$. Here, α is the specific-heat exponent; it is 0 for the 2D Ising model. The leading anomaly of the energy is $\alpha = 0$, although the specific heat, the temperature derivative of the energy, has logarithmic divergence. Using the critical energies for each size, we plot the left-hand side of (8), $\epsilon(T_c)/\coth(2J/T_c) + \epsilon(T_c^*)/\coth(2J/T_c^*)$, as a function of $1/L = 1/\sqrt{N}$ in figure 9. The result of polynomial fitting (on the second order in powers of $1/\sqrt{N}$) is also shown by the dotted curve. Then we obtain the estimate of the left-hand side of (8) as $\epsilon(T_c)/\coth(2J/T_c) + \epsilon(T_c^*)/\coth(2J/T_c^*) = 1.000 \pm 0.001$. We also evaluated the critical energies by the same fitting procedure as $E(T_c)/N = -1.319$ for the original lattice and $E(T_c^*)/N = -1.505$ for the dual lattice.

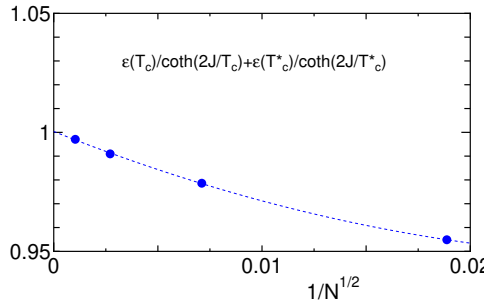


Figure 9. FSS of the critical energies of the Ising model on the Smith-kite lattices. We plot the left-hand side of (8) as a function of $1/L = 1/\sqrt{N}$. We also give the result of polynomial fitting by the dotted curve.

The present result clearly indicates that the duality relations for the critical temperature and the critical energy hold for an aperiodic monotile lattice. In the case of the Penrose lattice, Komura and Okabe [15] presented the analytical argument for the duality relation based on the discussion by Kramers and Wannier [19]. They followed a detailed argument by Syozi [24]. The point is that the duality relation comes from the local dual transformation of the lattice, not from the regularity of the lattice. Thus, the same story can be applied to the present Smith-kite aperiodic lattice.

3.3. Comparison with other lattices

Here, we compare the present results of the critical temperature with those of other lattices. For the Ising models on the Penrose lattice and its dual lattices, the estimates of the critical temperatures by a high-precision study [15] are

$$T_c^{\text{Penrose}} = 2.39781 \pm 0.00005 \quad (9)$$

and

$$T_c^{\text{dual Penrose}} = 2.14987 \pm 0.00005. \quad (10)$$

In the simulation of the high-precision study [15], the *periodic* Penrose lattice with a large unit cell was used. The formation of the Penrose tiling is associated with the golden ratio, which is the irrational number $\tau = (1 + \sqrt{5})/2$. The *periodic* Penrose lattice is

constructed by the continued-fraction expansion of the irrational number. The number of the lattice sites in the unit cell depend on the truncated level of the continued-fraction expansion.

It is also instructive to compare the present data with the data of regular lattices, where the coordination number is 4 on average. The critical temperatures of the Ising model on the kagome lattice and its dual lattice, the diced lattice, were exactly obtained [25, 26]. See also the calculation of the Fisher's zero for the kagome and diced lattices [27]. The obtained exact critical temperatures are

$$T_c^{\text{kagome}} = \frac{4}{\ln(3 + 2\sqrt{3})} = 2.143319\cdots \quad (11)$$

and

$$T_c^{\text{diced}} = \frac{2}{\cosh^{-1} \frac{1+\sqrt{3}}{2}} = 2.405457\cdots \quad (12)$$

Of course, these critical temperatures satisfy the duality relation (7).

In table 2, we compare the T_c 's of the Ising models on the (quasi-)lattices with the 4 coordination number. We also give the information on the lattice structure in table 2. The square lattice is self-dual, and we added it for reference;

$$T_c^{\text{square}} = \frac{2}{\ln(1 + \sqrt{2})} = 2.26919\cdots \quad (13)$$

The Smith-kite lattice, Penrose lattice, diced lattice are bipartite lattices, and take several values for the coordination number; there is no frustration for antiferromagnetic systems. On the other hand, the dual Smith-kite lattice, dual Penrose lattice, kagome lattice are not bipartite, and the coordination number is fixed as 4. Because there are “odd-numbered” rings, there appears frustration for antiferromagnetic systems. The duality relations are satisfied for all the dual pairs. The T_c 's of the Smith-kite lattice, Penrose lattice, diced lattice are almost the same, which reflects upon the similarity of the lattices.

4. Summary and discussions

To summarize, we have studied the Ising models on the Smith-kite lattice and the dual Smith-kite lattice by means of the SW multi-cluster spin-flip algorithm. We have estimated the critical temperatures on these lattices, and have shown that the finite-size scaling works quite well. The estimated critical temperature on the Smith-kite lattice is $T_c/J = 2.405 \pm 0.0005$ and that on the dual Smith-kite lattice is $T_c^*/J = 2.143 \pm 0.0005$. We have checked the duality relation. From the results of critical temperatures on the Smith-kite lattice and its dual lattice, we have obtained $\sinh(2J/T_c) \sinh(2J/T_c^*) = 1.000 \pm 0.001$. We have also shown the duality relation for the energy, $\epsilon(T_c)/\coth(2J/T_c) + \epsilon(T_c^*)/\coth(2J/T_c^*) = 1.000 \pm 0.001$. These numerical results clearly indicate that the duality relation is satisfied for an aperiodic monotile lattice. We have compared the present results with those of the Ising models on other

Table 2. Critical temperatures of Ising models on various (quasi-)lattices whose (average) coordination number is 4. We also give the information on the lattice structure in the table. The numbers in the parentheses are the average coordination number.

lattice	Smith-kite	d-Smith-kite	Penrose	d-Penrose
coordination number	3,4,6 (4)	4	3,4,5,6,7 (4)	4
bipartite	yes	no	yes	no
frustration (AF)	no	yes	no	yes
T_c/J	2.405	2.143	2.39781	2.14987
lattice	diced	kagome	square	
coordination number	3,6 (4)	4	4	
bipartite	yes	no	yes	
frustration (AF)	no	yes	no	
T_c/J	2.405457 ...	2.143319 ...	2.26919 ...	

lattices, including the Penrose lattice of quasicrystal and the regular lattices (kagome and dice lattices). The average coordination numbers of all these lattices are four.

We presented the results of $\text{Tile}(1, \sqrt{3})$ with 8 kites. We also performed the simulation for $\text{Tile}(\sqrt{3}, 1)$ with 10 kites. The results obtained are in close numerical agreement. Although not in perfect agreement, the difference is within 0.05% in the estimate of the critical temperatures. This can be attributed to the fact that both are tiling families of the same origin.

In the simulation of the Penrose lattice, the *periodic* lattice was used [13, 14, 15]. For the Smith-kite lattice, it will be helpful to use *periodic* lattice for high-precision simulation. Similar procedure to approximate the irrational number by a series of rational numbers could be applied to the case of Smith-kite lattice.

From the viewpoint of statistical physics, we have considered the Smith-kite lattice consisting of aperiodic monotiles. The study of electric systems, for example, on this aperiodic lattice is desirable. Quite recently, the spectral and transport properties of a tight-binding model defined on the Hat [28] and the dimer model on the Hat [29] have been discussed.

Finally, we would like to comment on the study of tiling itself. The aperiodic Smith tiling still has much to be studied from a mathematical science standpoint. The discovery of a new aperiodic monotile is also desirable.

Data availability statement

All data that support the findings of this study are included within the article.

Acknowledgments

We thank Arnaud Cheritat for allowing us to use the program code he created. This work was supported by JSPS KAKENHI Grant Number JP22K03472.

ORCID iDs

Yutaka Okabe <https://orcid.org/0000-0002-9434-5653>

References

- [1] Penrose R 1974 The role of aesthetics in pure and applied mathematical research *Bull. Inst. Math. Appl.* **10** 266
- [2] Levine D and Steinhardt P J 1984 Quasicrystals: A New Class of Ordered Structures *Phys. Rev. Lett.* **53** 2477
- [3] Shechtman D, Blech I, Gratias D and Cahn J W 1984 Metallic Phase with Long-Range Orientational Order and No Translational Symmetry *Phys. Rev. Lett.* **53** 1951
- [4] Smith D, Myers J S, Kaplan C S and Goodman-Strauss C 2023 An aperiodic monotile arXiv:2303.10798
- [5] Smith D, Myers J S, Kaplan C S and Goodman-Strauss C 2023 A chiral aperiodic monotile arXiv:2305.17743
- [6] Socolar J E S 2023 Quasicrystalline structure of the Smith monotile tilings arXiv:2305.01174
- [7] Baake M, Gähler F and Sadun L 2023 Dynamics and topology of the hat family of tilings arXiv:2305.05639
- [8] Akiyama S and Araki Y 2023 An alternative proof for an aperiodic monotile arXiv:2307.12322
- [9] Deguchi K, Nakayama M, Matsukawa S, Imura K, Tanaka K, Ishimasa T and Sato N K 2015 Superconductivity of Au-Ge-Yb Approximants with Tsai-Type Clusters *J. Phys. Soc. Japan* **84** 023705
- [10] Kamiya K, Takeuchi T, Kabeya N, Wada N, Ishimasa T, Ochiai A, Deguchi K, Imura K and Sato N K 2018 Discovery of superconductivity in quasicrystal *Nat. Commun.* **9** 154
- [11] Fuchs J N and Vidal J 2016 Hofstadter butterfly of a quasicrystal *Phys. Rev. B* **94** 205437
- [12] Nawa K, Avdeev M, Ishikawa A, Takakura H, Wang C W, Okuyama D, Murasaki R, Tamura R and Sato T J 2023 Magnetic properties of the quasicrystal approximant $\text{Au}_{65}\text{Ga}_{21}\text{Tb}_{14}$ *Phys. Rev. Mat.* **7** 054412
- [13] Okabe Y and Niizeki K 1988 Monte Carlo Simulation of the Ising Model on the Penrose Lattice *J. Phys. Soc. Japan* **57** 16
- [14] Okabe Y and Niizeki K 1988 Duality in the Ising Model on the Quasicrystals *J. Phys. Soc. Japan* **57** 1536
- [15] Komura Y and Okabe Y 2016 High-Precision Monte Carlo Simulation of the Ising Models on the Penrose Lattice and the Dual Penrose Lattice *J. Phys. Soc. Japan* **85** 044004.
- [16] Swendsen R H and Wang J S 1987 Nonuniversal critical dynamics in Monte Carlo simulations *Phys. Rev. Lett.* **58** 86
- [17] Hukushima K and Nemoto K 1996 Exchange Monte Carlo Method and Application to Spin Glass Simulations *J. Phys. Soc. Japan* **65** 1604
- [18] Cheritat A 2023 available at: <https://www.math.univ-toulouse.fr/~cheritat/AppletsDivers/Monotile-4D-lift/3-outlines/>
- [19] Kramers H A and Wannier G H 1941 Statistics of the Two-Dimensional Ferromagnet. Part I *Phys. Rev.* **60** 252
- [20] Binder K 1983 *Phase Transitions and Critical Phenomena* vol 8, ed C Domb and J Lebowitz (New York: Academic Press)
- [21] Binder K 1981 Finite size scaling analysis of ising model block distribution functions *Z. Phys. B: Condens. Matter* **43** 119
- [22] Barber M N 1983 *Phase Transitions and Critical Phenomena* vol 8, ed C Domb and J Lebowitz (New York: Academic Press)
- [23] Cardy J L 1988 *Finite Size Scaling* ed J L Cardy (Amsterdam: North-Holland)
- [24] Syozi I 1972 *Phase Transitions and Critical Phenomena* ed C Domb and M S Green (Academic Press, London) Vol. 1
- [25] Syozi I 1950 Statistics of Kagome Lattice *Prog. Theor. Phys.* **6** 306
- [26] Kano K and Naya S 1953 Antiferromagnetism. The Kagome Ising Net *Prog. Theor. Phys.* **10** 158
- [27] Feldmann H, Shrock R and Tsai S H 1998 Complex-temperature partition function zeros of the

Potts model on the honeycomb and kagome lattices *Phys. Rev. E* **57** 1335

- [28] Schirrmann J, Franca S, Flicker F and Grushin A G 2023 Physical properties of the Hat aperiodic monotile: Graphene-like features, chirality and zero-modes arXiv:2307.11054
- [29] Singh S and Flicker F 2023 Exact Solution to the Quantum and Classical Dimer Models on the Spectre Aperiodic Monotiling arXiv:2309.14447